Journal of Casting & Materials Engineering Vol. 5 No. 4 (2021) 84–88
https://doi.org/10.7494/jcme.2021.5.4.84

Set-up of a Generalized Dataset for Crack-Closure-Mechanisms of Cast Steel

Michael Horvath[a*], Matthias Oberreiter[a], Michael Stoschka[a], Martin Leitner[b]

[a] Montanuniversität Leoben, Christian Doppler Laboratory for Manufacturing Process based Component Design, Chair of Mechanical Engineering, Franz Josef-Straße 18, 8700 Leoben, Austria
[b] Technische Universität Graz, Institute of Structural Durability and Railway Technology, Inffeldgasse 25/D, 8010 Graz, Austria
**e-mail: michael.horvath@unileoben.ac.at*

Received: 20 August 2021/Accepted: 26 October 2021/Published online: 24 November 2021
This article is published with open access at AGH University of Science and Technology Journals

Paper presented at the EUROMAT 2021: Cast Irons and Steel Making. September 13–17, 2021, Virtual Conference.

Abstract

In components, crack propagation is subjected to crack-closure-mechanisms which affect the build-up of the relevant threshold stress intensity factor range during cyclic loading. As structural parts are exposed to service loads incorporating a variety of load ratios, a significant change of the long-crack threshold value occurs, leading to a severe stress ratio dependency of crack-closure-mechanisms. Thus, an extensive number of crack propagation experiments is required to gain statistically proven fracture mechanical parameters describing the build-up of closure effects as crack growth resistance curves.
The article presents a generalized dataset to assess the formation of crack-closure-mechanisms of cast steel G21Mn5+N. Numerous crack propagation experiments utilizing single edge notched bending (SENB) sample geometries are conducted, incorporating alternate to tumescent stress ratios. The statistically derived, generalized crack growth resistance curve features the impact of closure effects on the crack propagation rate in a uniform manner. To extend the dataset to arbitrary load ratios, the long-crack threshold approach according to Newman is invoked. The generalized dataset for the cast steel G21Mn5+N is validated by analytical fracture mechanical calculations for the utilized SENB-sample geometries. Incorporating a modified NASGRO equation, a sound correlation of analytical and experimental crack propagation rates is observed. Moreover, the derived master crack propagation resistance curve is implemented as a user-defined script into a numerical crack growth calculation tool and supports a local, node-based numerical crack propagation study as demonstrated for a representative SENB-sample. Concluding, the derived dataset facilitates the calculation of fatigue life of crack-affected cast steel components subjected to arbitrary stress ratios.

Keywords:

cast steel, crack propagation, fatigue life assessment, crack-closure-mechanisms, numerical crack growth simulation

1. INTRODUCTION

Cast steel is widely utilized in mechanical engineering applications to manufacture complexly shaped components with comparably high-strength in mass-production. As process parameters like the local solidification rate influence the microstructure of cast components extensively, manufacturing process-based imperfections, such as shrinkage porosities, slip bands or inclusions, occur during the solidification process [1]. These imperfections cause stress concentrations, which often act as crack initiation sites [2]. As the crack transits from short- to long-crack growth, propagation is heavily influenced by the build-up of mechanisms like plasticity- or roughness-induced crack-closure. These effects lead to an increase of the fatigue effective threshold stress intensity factor range, described as crack growth resistance curves [3]. This setting depends on microstructural material parameters as well as on the effective stress ratio, hence an extensive number of crack propagation experiments is required to conduct statistically valid fracture mechanical parameters that enable accurate fatigue life calculations of crack-afflicted cast steel components.

The following article presents a generalized dataset which describes the formation of crack-closure-mechanisms in the cast steel alloy G21Mn5+N. The dataset is validated by analytical crack propagation calculations of conducted SENB-sample experiments and is additionally implemented into a numerical crack propagation simulation tool. This not only features crack growth simulation studies for plain SENB-samples but also supports spatially shaped porosities under multiaxial loading.

2. EXPERIMENTAL WORK

To derive fracture mechanical parameters, crack propagation experiments are conducted on nine SENB-samples, with notch geometry as depicted in (Fig. 1).

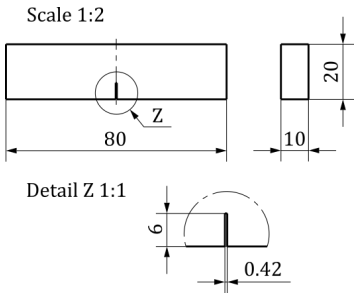

Fig. 1. SENB-specimen geometry for fracture mechanical testing

The chemical composition of the utilized cast steel alloy G21Mn5+N, as well as the static mechanical properties of the investigated material are summarized in [4]. After milling of the specimens from bulk material, an initial notch is manufactured utilizing wire-cut electrical discharge machining. Subsequently, the sides of the SENB-samples are polished in order to measure the initial notch geometry by light-optical microscopy. To achieve a defined pre-crack for the subsequent crack propagation experiments, the specimens are razor blade polished using diamond polishing suspension. A consecutive compressive pre-cracking procedure utilizing a SincoTec® Power Swing Mot tension-compression resonance test rig is conducted, followed by the measurement of the achieved pre-crack length a_0 of each specimen. The parameters of the razor blade polishing process, as well as the compressive pre-cracking, are based on a preceding master's thesis [5]. Finally, crack propagation investigations are performed on a RUMUL® Cracktronic resonance test rig. The specimens are subsequently tested under axial bending loading at various load ratios, see (Tab. 1). As recommended in [6], the test procedure utilizes a constant stepping of the cyclic stress intensity factor ΔK to increase the value of ΔK until long-crack propagation occurs.

The crack length is measured by the direct current potential drop method, incorporating a compensation of crack length fluctuations due to ambient temperature changes. A detailed description of the testing procedure is given in [7].

Table 1
SENB-samples with corresponding load ratios and pre-crack lengths

Specimen	R [–]	a_0 [mm]
GP1	0.000	7.148
GP2	0.500	6.695
GP3	–1.000	6.614
GP4	–1.000	6.479
GP7	–1.000	6.511
GP9	–1.000	6.730
GP26	0.000	6.548
GP28	0.500	6.877
L2U	0.000	6.523

3. DEVELOPMENT OF A GENERALIZED RESISTANCE CURVE

As the crack propagates from a short- to a long-crack, closure-effects occur due to the plastic zone surrounding the crack tip and the roughness of the growing crack's flanks. These mechanisms lead to an increase of the threshold stress intensity factor range $\Delta K_{th}(\Delta a)$, which is described by Equation (1) as proposed in [3].

$$\Delta K_{th}(\Delta a) = \Delta K_{th,eff} + \\ +\left(\Delta K_{th,lc} - \Delta K_{th,eff}\right)\cdot\left[1-\Sigma_{(i=1)}^{n}\nu_i exp-\left(\frac{\Delta a}{l_i}\right)\right] \quad (1)$$

where:

$\Delta K_{th}(\Delta a)$ – threshold stress intensity factor range [MPa√m],
$\Delta K_{th,eff}$ – intrinsic (effective) threshold stress intensity factor range [MPa√m],
$\Delta K_{th,lc}$ – long-crack growth threshold stress intensity factor range [MPa√m],
Δa – crack extension [mm],
ν_i – weighting factors [–],
l_i – fictitious length scales [mm].

In order to develop a generalized dataset for the description of crack-closure-mechanisms, the course of $\Delta K_{th}(\Delta a)$ is parametrized and compared to the experimental results by means of the least-mean-squares residual. Thereby, the weighting factors ν_i and the fictitious length scales l_i are evaluated. Incorporating the material intrinsic threshold stress intensity factor range $\Delta K_{th,eff}$ and the long-crack threshold stress intensity factor range $\Delta K_{th,lc}$, the specific resistance curve for the corresponding specimen can be calculated, as shown for specimen GP3 in (Fig. 2).

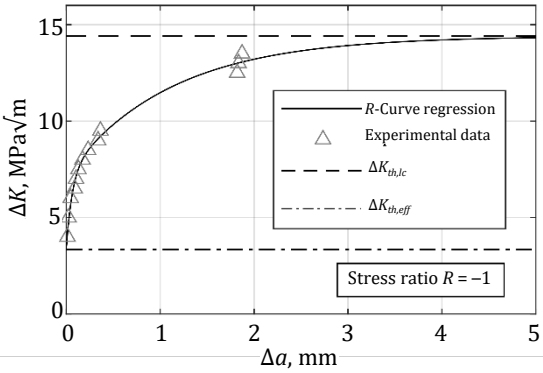

Fig. 2. Experimentally derived resistance curve of specimen GP3

In order to obtain generalized values for the weighting factors ν_i and the length scales l_i, the evaluated resistance curves are standardized by calculation of the dimensionless crack closure factor $f_{cl}(\Delta a)$, see Equation (2). This unification procedure is reasoned in [8].

$$f_{cl}(\Delta a) = \frac{\Delta K_{th}(\Delta a) - \Delta K_{th,eff}}{\Delta K_{th,lc} - \Delta K_{th,eff}} \quad (2)$$

As the evaluated crack closure factor f_{cl} depends on the crack extension Δa, another least-mean-squares regression loop is utilized to derive load ratio independent parameters v_i and l_i for the standardized dataset. Moreover, the experimentally derived crack propagation rate, the material and load ratio dependent parameters C, m and p are evaluated, which describe the crack propagation rate as a function of the cyclic stress intensity, utilizing a modified NASGRO-equation as presented in [3]. To complete the proposed generalized dataset, the load ratio dependency of the aforementioned parameters is finally studied and values for each parameter are evaluated. The C- and m-values depend on the load ratio and are in agreement with the common engineering guideline FKM (Forschungskuratorium Maschinenbau) [9]. The p-value can be set load ratio independent for a generalized fracture mechanical dataset.

3.1. Analytical crack growth calculation

To validate the established generalized dataset, first an analytical crack growth calculation is conducted. As already mentioned, the modified NASGRO-equation [3] is utilized which extends the calculation of the fatigue crack propagation rate da/dN towards short-crack growth, see Equation (3).

$$\frac{da}{dN} = C \cdot F \cdot \Delta K^m \cdot \frac{\left[1 - \frac{\Delta K_{th}(\Delta a)}{\Delta K}\right]^p}{\left[1 - \frac{K_{max}}{K_c}\right]^q} \tag{3}$$

where:

- da/dN – fatigue crack growth rate [nm/cycle],
- C – crack growth constant [(nm/cycle)/(MPa√m)^m],
- F – crack velocity factor [–],
- ΔK – stress intensity factor range [MPa√m],
- m – Paris exponent [–],
- p – empirical constant, which describes the curvature of the crack growth curve in the threshold region [–],
- q – empirical constant, which describes the curvature of the crack growth curve in the instability region [–],
- K_{max} – maximum stress intensity factor [MPa√m],
- K_c – fracture toughness [MPa√m].

Detailed information on the respective parameters and their dependencies, e.g. regarding the crack extension, is provided in [3]. As the experimental work focusses on the determination of acting crack-closure effects and the consequential build-up of the threshold stress intensity factor range, the law is not applied towards the instability crack growth region with stress intensities close to fracture toughness. Hence, the exponent q is purposely set to zero, implying non-conservative crack growth rates in the instability region. Considering that fatigue crack initiation and stable crack propagation constitutes the main portion of structural fatigue lifetime, the non-conservative treatment of the instability crack growth fraction is negligible.

The stress intensity factor range for a SENB-sample geometry under pure bending load is calculated according to [10], utilizing the loading conditions applied in the aforementioned SENB-experiments. Validation of the generalized dataset is conducted by analytical calculation of the crack growth rate and comparison to the experimentally derived values of da/dN, as depicted exemplarily for tumescent loading of specimen GP1 in (Fig. 3)

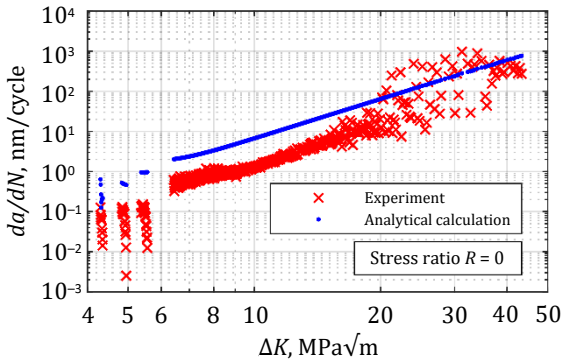

Fig. 3. Comparison of experimentally and analytically derived crack growth rates for SENB-specimen GP1

Utilizing the generalized dataset to consider crack-closure-mechanisms analytically, the calculated crack growth rates are somewhat conservative compared to the experimental results. Thus, the analytically determined accumulated fatigue lifetime only represents a fraction of the actual fatigue life. It should be noted that the invoked fracture mechanical parameters have been determined by regression of the crack growth resistance curves.

3.2. Optimization of generalized parameters

To improve the accuracy of the presented generalized dataset even further, the parameters included therein have been optimized in a consecutive parameter study by minimization of total fatigue lifetime as residual. By variation of the individual fracture mechanical parameters within a sensitivity study, the adapted generalized dataset shows a sound agreement with the experimental results, while retaining the conservative character of the initial proposal. The analytically evaluated crack growth rates utilizing the optimized parameter set are exemplarily depicted in (Fig. 4) for a representative specimen.

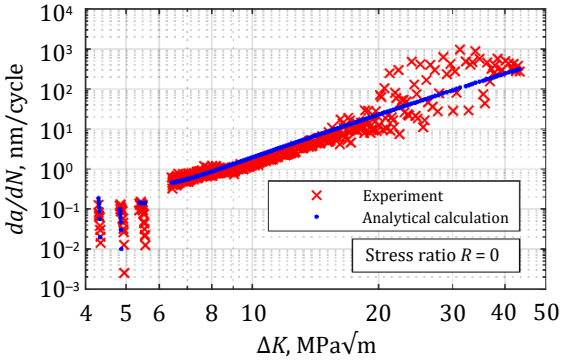

Fig. 4. Validation of the optimized parameter set by comparison of experimentally and analytically derived crack growth rates for SENB-specimen GP1

To extend the optimized dataset to arbitrary load ratios, the approach according to Newman [11, 12] is implemented as shown in (Fig. 5).

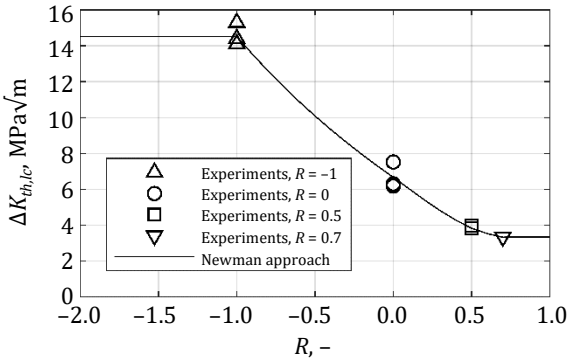

Fig. 5. Threshold stress intensity factor range as a function of the load ratio utilizing a Newman approach

Finally, the optimized fracture mechanical crack-closure dependent parameters of the generalized dataset incorporating arbitrary load ratios are listed in (Tab. 2).

Table 2
Generalized dataset for cast steel alloy G21Mn5+N

R [–]	l_1 [mm]	l_2 [mm]	ν_1 [–]	ν_2 [–]
–	0.075	2.000	0.450	0.550

The load ratio dependency of the parameters C, m and p has been evaluated for the conducted experiments and the corresponding values are depicted in (Tab. 3).

Table 3
Parameters C, m and p for selected load ratios

R [–]	C [(nm/cycle)/(MPa√m)^m]	m [–]	p [–]
−1.0	0.001	3.750	0.500
0.0	0.004	3.250	0.500
0.5	0.020	2.650	0.500

To improve statistical coverage of C-, m- and p-values for other load ratios, further experiments are scheduled.

3.3. Numerical implementation

The application of the derived generalized dataset in crack growth simulation is only demonstrated for specimen GP1, as depicted in (Fig. 6), utilizing FRANC3D® and a user-defined Python script. The test log determines the initial crack length. The cyclic load increment is fixed, leading to a threshold close to the corresponding experiment.

The numerically derived crack growth rates in (Fig. 6) show a sound agreement with the experimental results presented in (Fig. 4), supporting the fracture mechanical analyses of complexly shaped crack geometries, where no analytical formulation is yet reported. It should be noted that the numerical simulation supports a localized assessment of crack-closure effects by the presented generalized dataset.

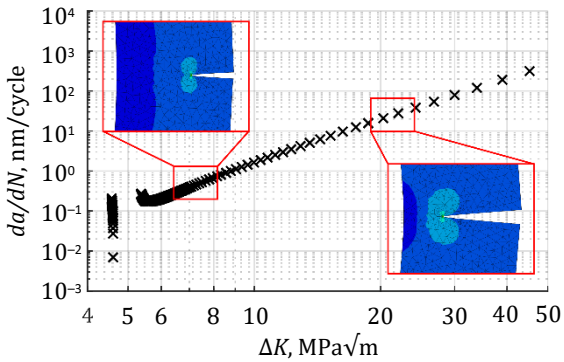

Fig. 6. Numerically evaluated crack growth rates utilizing the generalized dataset

4. SUMMARY

The present article proposes a generalized dataset for the description of crack-closure-mechanisms in G21Mn5+N for arbitrary load ratios. The analytical and numerical investigations conducted show a conservative calculation of the experimental lifetime results. Future work deals with the applicability of the dataset for other cast materials, such as high-strength cast steel alloys.

Acknowledgments

The financial support by the Austrian Federal Ministry for Digital and Economic Affairs and the National Foundation for Research, Technology and Development is gratefully acknowledged.

REFERENCES

[1] Campbell J. (2011). *Complete Casting Handbook*. Oxford, UK: Elsevier Butterworth-Heinemann.
[2] Collini L., Pirondi A., Bianchi R., Cova M. & Milella P.P. (2011). Influence of casting defects on fatigue crack initiation and fatigue limit of ductile cast iron. *Procedia Engineering*, 10, 2898–2903. Doi: https://doi.org/10.1016/j.proeng.2011.04.481.
[3] Maierhofer J., Pippan R. & Gänser H.-P. (2014). Modified NASGRO equation for physically short cracks. *International Journal of Fatigue*, 59, 200–207. Doi: https:doi.org/10.1016/j.ijfatigue.2013.08.019.
[4] Schuscha M., Leitner M., Stoschka M. & Meneghetti G. (2020). Local strain energy density approach to assess the fatigue strength of sharp and blunt V-notches in cast steel. *International Journal of Fatigue*, 132, 105334. Doi: https://doi.org/10.1016/j.ijfatigue.2019.105334.
[5] DeLuca F. (2020). *Experimental and theoretical analysis of crack propagation thresholds of metal materials*. Universita Degli Studi Di Padova [Master thesis].
[6] Tabernig B. & Pippan R. (2002). Determination of the length dependence of the threshold for fatigue crack propagation. *Engineering Fracture Mechanics*, 69(8), 899–907. Doi: https://doi.org/10.1016/S0013-7944(01)00129-1.
[7] Oberreiter M., Aigner R., Pomberger S., Leitner M. & Stoschka M. (2021). Impact of microstructural properties on the crack threshold of aluminium castings. *Engineering Fractue Mechanics*, 241, 107431. Doi: https://doi.org/10.1016/j.engfracmech.2020.107431.
[8] Kolitsch S., Gänser H.-P., Maierhofer J. & Pippan R. (2016). Fatigue crack growth threshold as a design criterion – statistical scatter and load ratio in the Kitagawa-Takahashi diagram. *IOP Conference Series: Materials Science and Engineering*, 119, 12015. Doi: https://doi.org/10.1088/1757-899X/119/1/012015.

[9] Berger C. (2009). *Fracture mechanics proof of strength for engineering components*. Frankfurt am Main: VDMA.
[10] Murakami Y. (2001). *Stress intensity factors handbook*. Kyoto: The Society of Materials Science, Japan.
[11] Newman J.C. (1984). A crack opening stress equation for fatigue crack growth. *International Journal of Fracture*, 24(4), R131–R135. Doi: https:doi.org/10.1007/BF00020751.
[12] Mettu S., Shivakumar V., Beek J., Yeh F., Williams L., Forman R., McMahon J. & Newman I. (1999). NASGRO 3.0: A software for analyzing aging aircraft. *The Second Joint NASA/FAA/DoD Conference on Aging Aircraft: August 31 – September 3, 1998. Williamsburg, Virginia,* 792–801. Hampton, Virginia: NASA Langley Research Center.